Inferring transcriptional regulators through integrative modeling of public chromatin accessibility and ChIP-seq data

Qian Qin[1,2,*], Jingyu Fan[1,*], Rongbin Zheng[1], Changxin Wan[1], Shenglin Mei[1], Qiu Wu[1], Hanfei Sun[1], Jing Zhang[3,4,+], Myles Brown[5,6], Clifford A. Meyer[5,7,+], X. Shirley Liu[1,5,7,+]

[1] Shanghai Key Laboratory of Tuberculosis, Clinical Translational Research Center, Shanghai Pulmonary Hospital, School of Life Sciences and Technology, Tongji University, Shanghai 200092, China

[2] Children's hospital of Fudan University, Center of Molecular Medicine, Shanghai 201102, China

[3] School of Life Science and Technology, Tongji University, Shanghai 200065, China

[4] Stem Cell Translational Research Center, Tongji Hospital, School of Life Science and Technology, Tongji University, Shanghai 200065, China

[5] Center for Functional Cancer Epigenetics, Dana-Farber Cancer Institute, Boston, Massachusetts 02215, USA

[6] Department of Medical Oncology, Dana-Farber Cancer Institute, Harvard Medical School, Boston, Massachusetts 02215, USA

[7] Department of Data Sciences, Dana-Farber Cancer Institute and Harvard T.H. Chan School of Public Health, Boston, Massachusetts 02215, USA

[*] These authors contributed equally to this work and can interchangeably be ordered as co-first author.

[+] Corresponding authors: **cliff_meyer@ds.dfci.harvard.edu**, **xsliu@ds.dfci.harvard.edu**, **zhangjing@tongji.edu.cn.**

Abstract

We developed Lisa (http://lisa.cistrome.org) to predict the transcriptional regulators (TRs) of differentially expressed or co-expressed gene sets. Based on the input gene sets, Lisa first uses compendia of public histone mark ChIP-seq and chromatin accessibility profiles to construct a chromatin model related to the regulation of these genes. Then using TR ChIP-seq peaks or imputed TR binding sites, Lisa probes the chromatin models using *in silico* deletion to find the most relevant TRs. Applied to gene sets derived from targeted TF perturbation experiments, Lisa boosted the performance of imputed TR cistromes, and outperformed alternative methods in identifying the perturbed TRs.

Keywords

Transcription factors, gene regulation, chromatin accessibility, DNase-seq, H3K27ac ChIP-seq, differential gene expression, gene set analysis

List of abbreviations

TF: transcription factor

CR: chromatin regulator

TR: transcriptional regulator
RP: regulatory potential
ISD: in silico deletion
ROC: receiver operator characteristic
AUC: area under curve
ChIP-seq: chromatin immunoprecipitation followed by DNA sequencing
DNase-seq: DNase I digestion followed by DNA sequencing
H3K27ac: histone H3 lysine 27 acetylation
AR: Androgen Receptor
ER: Estrogen Receptor
GR: Glucocorticoid Receptor

Introduction

Transcriptional regulators (TRs), which include transcription factors (TFs) and chromatin regulators (CRs), play essential roles in controlling normal biological processes and are frequently implicated in disease[1-4]. The genomic landscape of TF binding sites and histone modifications collectively shape the transcriptional regulatory environments of genes[5-8]. ChIP-seq has been widely used to map the genome-wide set of cis-elements bound by trans-acting factors such as TFs and CRs, which we henceforth refer to as "cistromes"[9]. There are approximately 1,500 transcription factors in human and mouse[10,11], regulating a wide variety of biological processes in constitutive or cell-type-specific manners, and tens of thousands of ChIP-seq and DNase-seq experiments have been performed in human and mouse. We previously developed the Cistrome Data Browser (DB)[12], a collection of uniformly processed TF ChIP-seq (~11,000) and chromatin profiles (~12,000 histone mark ChIP-seq and DNase-seq) in human and mouse.

The question we address in this paper is how to effectively use these data to infer the TRs that regulate a query gene set derived from differential or correlated gene expression analyses in human or mouse. TR ChIP-seq data, when available, is the most accurate available data type representing TR binding. ChIP-seq data availability, in terms of covered TRs and cell types, even with large contributions from projects such as ENCODE[13], is still sparse due to the limited availability of specific antibodies. Although advances have been made in TR cistrome mapping with the introduction of technologies such as CETCh-seq[14] and CUT & RUN[15], the difficulties in acquiring TR ChIP-seq data for new factors limit the TR by cell type coverage of high quality TR ChIP-seq data. Chromatin accessibility data, including DNase-seq[16,17] and ATAC-seq[18], is

available for hundreds of cell types and provides maps of the regions in which TRs are likely to be bound in the represented cell types. The H3K27ac histone modification, associated with active enhancers and promoters of actively transcribed genes, has been widely profiled using ChIP-seq in many cell types[5,19]. When TF ChIP-seq data is not available, TF binding motifs, used in combination with chromatin accessibility data or H3K27ac ChIP-seq data might be used to infer TF binding sites[7,20,21]. Machine learning approaches that transfer models learnt from TF ChIP-seq peaks, motifs and DNase-seq data between cell types are promising ways of imputing TF cistromes, although imputation of TF binding sites on a large scale remains to be implemented[22-27]. Computationally imputed TF binding data is expected to represent TF binding sites less accurately than TF ChIP-seq experimental data, so we sought to develop a TR prediction method that could use imputed TF cistromes effectively, along with ChIP-seq derived ones.

We previously developed MARGE to characterize the regulatory association between H3K27ac ChIP-seq and differential gene expression in terms of a regulatory potential (RP) model[28]. The RP model provides a summary statistic of the cis-regulatory influence of the many cis-regulatory elements that might influence a gene's transcription rate. MARGE builds a classifier based on H3K27ac ChIP-seq RPs from the Cistrome DB to discriminate the genes in a query differentially expressed gene set from a set of background genes. One of the functions of MARGE is to predict the cis-regulatory elements (*i.e.* genomic intervals) that regulate a gene set. BART[29] extends MARGE, to predict the TRs that regulate the query gene set through an analysis of the predicted cis-regulatory elements. Here we describe Lisa (the second descendent of MARGE), a more accurate method of integrating H3K27ac ChIP-seq and DNase-seq with TR ChIP-seq or imputed TR binding sites to predict the TRs that regulate a query gene set. Unlike BART, Lisa does not carry out an enrichment analysis of the cis-regulatory elements predicted by MARGE. Instead, Lisa analyses the relationship between TR binding and the gene set using RP models and RP model perturbations. We assessed the performance of Lisa and other TR identification methods, BART[29], i-CisTarget[30] and Enrichr[31] using differentially expressed gene sets derived from experiments in which the activities of specific TFs were perturbed by knockdown, knockout, over-expression, stimulation or inhibition.

Results and Discussion

Regulatory TR prediction based on Cistrome DB ChIP-seq peaks

High quality TR ChIP-seq data, when available, accurately characterizes genome-wide TR binding sites, which can be used to infer the regulated genes in particular cell types. Estimating the effect of TR binding on gene expression is not trivial because: (1) there is no accurate map linking enhancers to the genes they regulate[32], (2) multiple enhancers can regulate the same gene[33] and a single enhancer can regulate multiple genes[34] and (3) not all TR binding sites are functional enhancers[19]. A model is therefore needed to quantify the likelihood of a gene being regulated by a TR cistrome. The "peak-RP" model[35,36] is based on TR ChIP-seq peaks, serving as a proxy for TR binding sites, without the use of DNase-seq or H3K27ac ChIP-seq data. In the peak-RP model (Fig. 1a) the effect a TR binding site has on the expression of a gene is assumed to decay exponentially with the genomic distance between the TR binding site and the TSS, and the contribution of multiple binding sites is assumed to be additive[36]. Accounting for the number of TR binding sites and for the distances of these sites from the TSS has been shown to be more accurate than alternative TR target assignment methods[37]. While it is possible that enhancers could modulate each other in non-additive ways[32], data on these types of behavior are too scarce to incorporate in a TR prediction model.

We use the peak-RP model to identify TFs that are likely regulators of a target gene set by searching for Cistrome DB[12] cistromes that produce higher peak-RPs for the query gene set than for a set of background genes (Supp. Fig. 1, Supp. Table 1). Statistical significance is calculated using the one-sided Wilcoxon rank-sum test statistic comparing the peak-RPs for the query gene set with the background. The TRs with the most significant p-values are considered to be the candidate regulators. Lisa uses TR ChIP-seq within the peak-RP model, along with the chromatin landscape models described below to infer the TRs of a gene set.

Regulatory TR prediction using a chromatin landscape model

While TR ChIP-seq data provides accurate information about TR cistromes in specific cell types, the Cistrome DB TR by cell type coverage is skewed towards a few TRs, such as CTCF, which are represented in many cell types, and towards cell types such as K562 (Supp. Fig. 1b-c), in which many TRs have been characterized (Supp. Fig. 1d). H3K27ac ChIP-seq[19] and DNase-seq[16], available in a large number and variety of cell types, can be used to infer cell type specific regulatory regions. These types of data could enhance the use of TR ChIP-seq data as well as imputed TF binding data, which may not accurately represent TF binding sites in different cell contexts.

To boost the performance of TF ChIP-seq or imputed TF binding data in the identification of regulatory TRs, we developed Lisa chromatin landscape models, which use H3K27ac ChIP-seq and DNase-seq chromatin profiles (Fig. 1b, Supp. Table 2, and Methods) to model the regulatory importance of different genomic loci. As differential gene expression experiments are not always carried out in parallel with chromatin profiling experiments, Lisa does not require the corresponding user-generated chromatin profiles, but instead uses the DNase-seq and H3K27ac ChIP-seq data that is available in the Cistrome DB to help identify cis-regulatory elements controlling a differential expression gene set. To this end, Lisa models chromatin landscapes through chromatin RPs (chrom-RPs, Fig. 1b), which are defined in a similar way to the peak-RP with one small difference: genome-wide read signals instead of peak calls are used in the calculation of the chrom-RP[28]. Changes in H3K27ac ChIP-seq and DNase-seq associated with cell state perturbations are often a matter of degree rather than switch-like, therefore we base the chrom-RP on reads rather than peaks. The chrom-RP is pre-calculated for each gene (Fig. 1c-1) and for each H3K27ac ChIP-seq / DNase-seq profile in the Cistrome DB (Supp. Fig. 1a, Supp. Table 2). These chrom-RPs quantify the cis-regulatory activities that influence each gene under cell-type specific conditions.

Given the query gene set, Lisa identifies a small number of Cistrome DB DNase-seq and H3K27ac ChIP-seq samples that are informative about the regulation of these genes. Lisa does this by using the pre-calculated H3K27ac / DNase-seq chrom-RPs to discriminate between the query gene set and a background gene set. Using L1-regularized logistic regression, Lisa assigns a weight to each selected sample so the weighted sum of chrom-RPs on the genes best separates the query and the background gene sets (Fig. 1c-2). This step is carried out separately for H3K27ac ChIP-seq and DNase-seq, yielding a chrom-RP model based on H3K27ac ChIP-seq and another model based on DNase-seq.

Next, by a process of *in silico* deletion (ISD), Lisa evaluates the effect deleting each TR cistrome has on the chromatin landscape model (Fig. 1c-3). ISD of a TR cistrome involves setting DNase-seq or H3K27ac ChIP-seq chromatin signal to zero in the 1kb intervals containing the peaks in that cistrome and evaluating the effect on the predictions made by the chromatin landscape models. The difference of the model scores before ISD and after ISD quantifies the impact that the deleted TR cistrome is predicted to have on the query and background gene sets. Lisa does not make a prediction of cis-regulatory elements, the approach taken by MARGE and BART. Instead, Lisa probes the effects of deleting putative regulatory TR cistromes on the chrom-RP

model. Whereas the chrom-RP integrates data over 200kb intervals, the scale of individual cis-regulatory elements is of the order of 1kb. The ISD approach mitigates the difficulties in transferring information contained in the chrom-RP model from the chrom-RP (200kb) scale to the cis-regulatory element (1kb) scale.

Finally, to prioritize the candidate TRs, Lisa compares the predicted effects on the query and background gene sets using the one-sided Wilcoxon rank-sum test (Fig. 1c-4). A one-sided test is used because Lisa assumes that the *in silico* deletion of a true regulatory factor will decrease, not increase, the model's ability to discriminate between query and background gene sets. To utilize the power of predictions based on H3K27ac-ChIP-seq and DNase-seq ISD models, and TF ChIP-seq peak-only models (Fig. 1c-5), results are combined using the Cauchy combination test[38] (Fig. 1c-6). Whereas MARGE[28] predicts cis-regulatory elements (but does not analyze TRs), and BART[29] carries out an enrichment analysis of predicted cis-elements to discover TRs, Lisa uses the chromatin landscape model in a different way. In combination with ChIP-seq-derived or computationally imputed TR binding, Lisa probes the effects of TRs on the chromatin RP models of query and background gene sets.

Demonstration of chromatin landscape models in a GATA6 knock-down study

We demonstrate Lisa chromatin landscapes and *in silico* deletion using a query gene set defined as the down-regulated genes in a GATA6 knock-down experiment in the KATO-III stomach cancer cell line[39] (Fig. 2). Lisa identifies DNase-seq and H3K27ac ChIP-seq chromatin landscape models (Fig. 2a, Fig. 1c-2), which include several gastro-intestinal samples (Supp. Fig. 2b,d) whose chrom-RPs can discriminate between the query and background gene sets (Supp. Fig. 2a, DNase-seq ROC AUC=0.816, Supp. Fig. 2c, H3K27ac ROC AUC=0.821). *In silico* deletion (Fig. 1c-3) of GATA6 binding sites produces larger DNase-seq and H3K27ac ΔRPs (DNase ΔRP: 1.05, H3K27ac ΔRPs: 0.25) for an example down-regulated gene, *LINC01133*[40], than for a background gene, *ZC3H12A* (DNase ΔRP: 0.06, H3K27ac ΔRP: 0.01) (Fig. 2b). *In silico* deletion of CTCF binding sites, in contrast, has a smaller effect on the chromatin landscapes surrounding *LINC01133* (DNase ΔRP: 0.02, H3K27ac ΔRP: 0.01), resulting in ΔRPs that are more similar to the ΔRPs for *ZC3H12A* (Fig. 2b) (DNase ΔRP: 0.004, H3K27ac ΔRP: 0.001). Statistical analysis is carried out comparing all the query gene ΔRPs with all the background gene ΔRPs (Fig 1c-4), producing significant p-values for GATA4 (DNase p-val < 10^{-10}, H3K27ac p-val < 10^{-5}) and GATA6 (DNase p-val < 10^{-13}, H3K27ac p-val < 10^{-7}). After this analysis is conducted for all TR ChIP-seq

samples in the Cistrome DB and the results are combined and compared, GATA6 and GATA4 ChIP-seq from intestinal and gastric tissues have the most significant p-values Fig. 2c,d).

Lisa identification of regulatory TF ChIP-seq sample clusters

To investigate whether a TF ChIP-seq cistrome derived from one cell type can be informative about other cell types, we first clustered all the human TR cistromes in the Cistrome DB based on the pairwise Pearson correlation of peak-RP scores as a heatmap (Fig. 3). We then applied Lisa to differentially expressed gene sets defined by perturbations of individual TFs and examined the TR cistromes predicted to be the key regulators of these gene sets. In the analysis of up-regulated genes on Androgen Receptor (AR) activation in the LNCaP prostate cancer cell line, Lisa identified a tight cluster of significant cistromes for AR and its known collaborator FOXA1 (Fig. 3a). All samples in this cluster were derived from prostate cancer cell lines. In the analysis of the GATA6 knock-down in the gastric cancer cell line (KATO-III), Lisa found the GATA6 and FOXA2 cistromes in stomach and colon samples to be the most significant. FOXA2 is an important pioneer TF which has been reported to collaborate with GATA6 in gut development to regulate Wnt6[41] and Wnt7b[42] (Fig. 3b). The identification of GATA6 cistromes in colon cancer cell lines, in addition to gastric cancer cell lines, shows that cistromes derived from cell types that are of related lineages can be used to inform the identification of the relevant regulators, even if the cell types are not the same. In the third example involving Glucocorticoid Receptor (GR) activation in the lung cancer cell line A549, Lisa correctly identified GR in A549 as a likely regulator, and also identified GR in a different cell type HeLa (Fig. 3c). AR, a member of the same nuclear receptor family as GR, is also implicated by Lisa even though the AR cistrome samples do not cluster with GR cistrome samples and have less statistical significance.

We carried out an analysis of the effects of removing ChIP-seq and DNase-seq data on Lisa's accuracy. In particular, we tested Lisa's performance on three up-regulated gene sets: (1) GR activated genes in breast cancer (MCF7), (2) GR activated genes in lung cancer (A549), and (3) Estrogen Receptor (ER) activated genes in MCF7 (Supp. Table 3). In these analyses we assessed the effect of removing all relevant cell line specific (MCF7 or A549), H3K27ac ChIP-seq and DNase-seq data, or cell line specific TR ChIP-seq data (ER or GR). We also removed cell line specific TR ChIP-seq data together with H3K27ac ChIP-seq and DNase-seq data. We repeated the same analysis removing similar data, on the basis of tissue (breast and lung) instead of on the basis of cell line (MCF7 and A549). When MCF7 ER ChIP-seq are excluded, an ER sample from another breast cancer cell line (H3396) predicts the importance of ER (rank 6) as a regulator

of the estrogen activated gene set. When all ER breast ChIP-seq samples are excluded, Lisa can still identify ER (rank 18) from ER ChIP-seq in the VCaP prostate cancer cell line. For the GR activated gene set in MCF7, when GR ChIP-seq data is unavailable in MCF7, Lisa can identify GR as a key regulator (rank 2) using GR ChIP-seq from lung (A549). For the GR activated gene set in lung, Lisa identified GR as the key regulator (rank 1) using GR ChIP-seq data from breast (MDA-MB-231). Together, these observations indicate that although TRs often bind in cell type dependent ways, ChIP-seq derived TR cistromes can be informative about the gene sets that TRs regulate in some other cell types.

Lisa identification of TF associated cofactors in addition to TFs

To illustrate Lisa's capacity to find cofactors that interact with the regulatory TFs, we examined the Lisa analyses of four differentially expressed gene sets derived from experiments involving the activation of GR[43] and the knock-down/out of BCL6[44], MYC[45], and SOX2[46]. Lisa analysis of GR activation in lung cancer ranked GR itself as the most significant TR for the up-regulated gene sets (Fig. 4a), and highly ranked pioneer TFs FOSL2 and CEBPB, which were down-regulated after GR activation (Fig. 3c). BCL6, a predominantly repressive TF, is a driver of diffuse large B-cell lymphoma (DLBCL)[47]. Lisa analysis of the up-regulated genes in a BCL6 knock-down experiment in a DLBCL cell line ranked BCL6 as the most significant TR for this gene set (Fig. 4b). Lisa also identified NCOR1 and NCOR2, which are transcriptional BCL6 corepressors involved of the regulation of germinal center[48-50]. SPI1, which recruits BCL6[51], and BCOR, another BCL6 corepressor[52], were ranked among the top TRs for the up-regulated gene set. In a MYC knock-down experiment in medulloblastoma, MYC and its dimerization partner, MAX[53], were among the top predicted regulators of the down-regulated genes (Fig. 4c). The histone methyltransferase, KDM2B, known to physically interact with MYC and to augment MYC-regulated transcription[54], was also detected among the top regulators. In the SOX2 knock-out experiment[2], NANOG, SOX2 and POU5F1, the key regulators of pluripotency, were the top predicted regulators of the down-regulated genes (Fig. 4d). Lisa also discovered a similar set of TRs for the gene set derived from a POU5F1 knockdown experiment in embryonic stem cells (Supp. Fig. 3,4a). In addition, β-catenin (CTNNB1), which interacts with SOX2 and is oncogenic in $SOX2^+$ cells[55], also ranked high for the down-regulated genes. The predicted regulators of the up-regulated genes in this experiment include FOXA1 and EOMES. FOXA1 is involved in early embryonic development[56], and has been observed to repress NANOG directly[57]. FOXA1 has been shown through co-immunoprecipitation to physically interact with SOX2[58]. SOX2, known to bind to an enhancer regulating EOMES in human ESCs, when knocked down triggers EOMES

expression and induces endoderm and trophectoderm differentiation[59]. Thus, in many cases, the known interactors are highly ranked along with the target activator or repressor. This suggests that even though the available TF ChIP-seq data in different cell types are sparse (Supp. Fig. 1d), Lisa can provide insights on possible regulatory TFs since transcriptional machinery tends to be organized in modules of interacting factors[60] (Supp. Fig. 4d).

Systematic evaluation of regulator prediction

To systematically evaluate Lisa, we compiled a benchmark panel of 122 differentially expressed gene sets from 61 studies involving the knock-down, knock-out, activation or over-expression of 27 unique human target TFs. In addition, we compiled 112 differentially expressed gene sets derived from 56 studies with 25 unique TF perturbations in mouse (Supp. Table 4, see “galleries” at http://lisa.cistrome.org). The full Lisa model was separately applied to the up-regulated and down-regulated gene sets in each experiment. We also carried out analyses of these gene sets using subcomponents of Lisa: the peak-RP method, as well as H3K27ac ChIP-seq and DNase-seq assisted ISD analyses. The putative regulatory cistromes were defined using either ChIP-seq peaks or from TF motif occurrence in the inferred chromatin models. The results allowed us to compare the effectiveness of DNase-seq and H3K27ac ChIP-seq in scenarios where the TF cistromes are well estimated (by ChIP-seq) or less well estimated (by motif). We measured the performance based on their ranking of the perturbed target TF (Fig. 5, Supp. Fig. 5).

We compared the performance of methods that use TF ChIP-seq data and TF motifs, on up- and down- regulated gene sets, and on over-expression / activation and knock-down / knock-out samples (Fig. 5a). In over-expression studies, the prediction performance of all methods tended to be better for the up-regulated gene sets, than for the down-regulated ones. The reverse is evident in the knock-out and knock-down studies for which the prediction performances are better for the down-regulated gene sets (Fig. 5b,c). This suggests that most of the TFs included in the study have a predominant activating role in the regulation of their target genes, under the conditions of the gene expression experiments, allowing these TFs to be more readily identified with the corresponding direction of primary gene expression response. Similar performance patterns were observed in the mouse benchmark datasets (Supp. Fig. 5). The performances of Lisa using ISD of TR ChIP-seq peak from chromatin landscapes were similar to the TR ChIP-seq peak-RP method, but outperformed motif-based methods by large margins.

To determine whether differences between up- and down-regulated gene sets could be explained by direct or indirect modes of TR recruitment, we studied two experiments involving ER and GR activation in greater detail. We defined "direct" ER and GR binding sites as ER/GR ChIP-seq peaks on genomic intervals containing the cognate DNA sequence elements, and "indirect" ER and GR binding sites as ER/GR ChIP-seq peaks without the sequence elements. Comparing direct and indirect binding sites in the respective ER and GR activation experiments (Supp. Fig. 6) we found that the up-regulated gene sets were more significantly associated with the direct binding sites (ER p-value: $1.5x10^{-15}$, GR p-value: $1.5x10^{-18}$) than with the indirect ones (ER p-value: $3.8x10^{-4}$, GR p-value: $1.4x10^{-12}$). The down-regulated gene sets were more significantly associated with the indirect binding sites (ER p-value: $1.5x10^{-15}$, GR p-value: $1.5x10^{-11}$) than with the direct ones (ER p-value: $4.6x10^{-2}$, GR p-value: $3.0x10^{-3}$).

In some cases, the perturbation of a TR may trigger stress, immune or cell cycle checkpoint responses that are not directly related to the initial perturbation. In the Lisa analysis of up-regulated genes after 24 hours of estradiol stimulation (GSE26834), for example, E2F4 is the top ranked TR, followed by ER. Estrogen is known to stimulate proliferation of breast cancer cells via a pathway involving E2F4, a key regulator of the G1/S cell cycle checkpoint[61]. In this case, Lisa might be correctly detecting a secondary response to the primary TR perturbation.

Comparison of Lisa with published methods

We next compared Lisa with other approaches, including BART[29], iCisTarget[30] and Enrichr[31], which can use either TR ChIP-seq data or motifs. We also included a baseline method that ranks TRs by comparing query and background gene sets based on the TR binding site number within 5kb centered on the TSS. Lisa outperformed BART, iCisTarget and Enrichr in terms of the percentage of the target TR identified within the top 10 across all the experiments, either using TF binding sites from ChIP-seq data or motif hits (Fig. 6a,b). Lisa uses a model based on chromatin data to give more weight to loci that are more likely to influence the expression of the query gene set. In this way Lisa improves the performance of TR inference with noisy cistrome profiles such as those imputed from DNA sequence motifs. In addition to being more accurate than other methods in terms of TR prediction, the Lisa web server (lisa.cistrome.org) has several unique features which allow investigators to explore relevant ChIP-seq data in ways that are not available in other applications.

Lisa Web Site and Gallery of Lisa's Benchmark Data

The Lisa web site (lisa.cistrome.org) displays two tables of results for each query gene set. The first summarizes the Lisa analysis based on TR ChIP-seq data, the second displays the Lisa analysis of TF binding sites imputed from DNA binding motifs. The ChIP-seq data table displays up to 5 ChIP-seq samples for each TR. Users can sort results by p-value and inspect metadata and quality control statistics for each of the ChIP-seq samples to understand whether the predictive samples may be derived from particular cell types or experimental conditions. Lisa provides quality control metrics, metadata, publication and read data repository links for the ChIP-seq data of putative regulatory TRs. Through Lisa, the ChIP-seq signal tracks can be viewed on the WashU Epigenome Browser[62]. Although the motif imputation-based analysis tends to be less accurate than the ChIP-seq based analysis, motifs can indicate roles for regulatory TRs for which ChIP-seq data is not widely available. Lisa's analysis of all the benchmark gene sets is also viewable on the Lisa web site. Users can explore these analyses to understand the 'typical' results of the analysis. Robust methods combined with visualization and data exploration features make Lisa a valuable tool for analyzing gene regulation in human and mouse.

Conclusion

In this study, we describe an approach for using publicly available ChIP-seq and DNase-seq data to identify the regulators of differentially expressed gene sets in human and mouse. On the basis of a series of benchmarks we demonstrate the effectiveness of our method and report recurrent patterns in the TRs predicted by these methods. We find the regulators of the up-regulated genes and the down-regulated ones are often different from each other, therefore in any analysis of differential gene expression, up- and down-regulated gene sets ought to be distinguished. Our results show that many TFs have a preferred directionality of effect, indicative of a predominant repressive or activating function. It is well known that many TFs can recruit both activating and repressive complexes[63], so the observed direction may be related to the stoichiometry and affinity of the activating or repressive cofactors. We also observe differences between ChIP-seq based analysis and motif based ones, suggesting differences in TF activity depending on whether a TF interacts directly with DNA or whether it is recruited via another TF[64]. When a TF is recruited by another TF it is likely that the enhancer has been already established by other TFs and protein complexes. Thus, the co-binding enhancer information of multiple TFs allows Lisa to identify both the DNA bound TFs and their partners which might not directly bind DNA.

Lisa's accuracy in predicting the regulatory TRs of a gene set depends on the perturbation used in the production of the differential gene expression data, the quality of the gene expression data,

the availability and quality of the DNase-seq, H3K27ac and TR ChIP-seq data sets, the degree to which binding is dependent on a DNA sequence motif, as well as the validity of the model assumptions. Although we evaluate Lisa using differential gene expression data associated with a TR perturbation, the perturbed TR might not be the main regulator of the gene set. For example, perturbation of a TR may trigger a stress response[65], or secondary transcriptional effects that are not directly related to the primary TR[66].

The modelling approach used in Lisa facilitates the prediction of regulatory TRs using available ChIP-seq and DNase-seq data. DNase-seq and H3K27ac ChIP-seq are available in a broad variety of cell types and these data are informative about cis-regulatory events mediated by many TRs. Although H3K27ac is considered to be a histone modification associated with gene activation Lisa can still identify TRs, such as BCL6 and EZH2, with predominantly repressive functions. Although Lisa uses the correlation between H3K27ac or chromatin accessibility and gene expression to predict regulatory TRs we do not assume that H3K27ac or chromatin accessibility cause the transcriptional changes. Other genomics data types that are predictive of general cis-regulatory activity, when available in quantity, variety and quality, might improve Lisa's performance. More importantly, high quality TR specific binding data, generated by ChIP-seq or alternative technologies, like CETCh-seq[14] or CUT & RUN[15], will be needed to improve Lisa's accuracy in predicting TRs that are not yet well represented in Cistrome DB. TR imputation methods might fill in some gaps in TR binding data, however, families of TRs such as homeobox and forkhead factors, which have similar DNA binding motifs can be hard to discriminate based on DNA sequence analysis.

Although Lisa aims to identify the regulators of any differentially expressed gene set in human or mouse, no matter the contrast, in practice, the query gene sets should be derived from biologically meaningful differential expression or co-regulation analyses. In this study, we based the methods evaluation on data from available TR perturbation experiments, which are biased towards well studied systems. For this reason, the reliability of methods based on TR ChIP-seq data may be overestimated relative to imputation-based methods because the available TR ChIP-seq data tends to be derived from similar cell types and for the same factors used in the gene perturbation experiments. When the relevant cell type specific TR ChIP-seq data is available the performance of the peak RP-method and ISD methods are similar, but when TR ChIP-seq data is not available, methods based on imputed TR cistromes are obligatory. The value of imputed cistromes relative to ChIP-seq derived ones will depend on the quantity, variety and quality of available ChIP-seq

data, the accuracy of the imputed cistromes, the degree of commonality of the genes that are regulated by the same TR in different cell types, and the number of TRs recognizing similar DNA sequence elements. Lisa provides invaluable information about the regulation of gene sets derived from both bulk and single cell expression profiles[67], and will become more accurate over time with greater coverage of TF ChIP-seq augmented by computationally imputed TF cistromes.

Methods

Preprocessing of chromatin profiles

Using the BigWig format signal tracks of human and mouse H3K27ac ChIP-seq and DNase-seq from Cistrome DB, we precomputed the chromatin profile regulatory potential (chrom-RP) of each RefSeq gene and also summarized the signal in 1kb windows genome-wide. The chrom-RP for gene k in sample j is defined as $R_{jk} = \sum_{i\in[t_k-L,\, t_k+L]} w_i s_{ji}$ (as defined in the MARGE algorithm[28]). L is set to 100kb, and w_i is a weight representing the regulatory influence of a locus at position i on the TSS of gene k at genomic position t_k, $w_i = 2e^{-\mu d}/1 + e^{-\mu d}$, where $d = |i - t_k|/L$, and i stands for i^{th} nucleotide position within the [-L,L] genomic interval centered on the TSS at t_k. s_{ji} is the signal of chromatin profile j at position i. μ is the parameter to determine the decay rate of the weight, which is defined as $\mu = -\ln {}^{L}/_{3\Delta}$. For DNase-seq and H3K27ac ChIP-seq, the decay distance Δ is set to 10kb. The genome-wide read counts on 1kb windows were calculated using the UCSC utility bigWigAverageOverBed[68]. The chrom-RP matrix for chromatin profiles was normalized across RefSeq genes within one chromatin profile by $R'_{jk} = \log(R_{jk}+1) - \frac{1}{k}\sum_1^k(\log(R_{jk}+1))$.

Preprocessing of cistromes

Using all human and mouse transcription regulator (TR) ChIP-seq cistromes peak BED files from the Cistrome Data Browser (v.1). We precomputed the TR binding sites based on ChIP-seq and motif hits based on position weight matrices then transferred as binary values at a 100bp resolution genome-wide. The DNA sequence scores were derived from Cistrome motifs, a redundant collection of 1,061 PWMs from TRANSFAC[69], JASPAR[70] and Cistrome DB ChIP-seq that includes 675 unique TFs in human and mouse. The peak based regulatory potential (peak-RP) of a TR cistrome is defined in the same way as the chrom-RP except s_i represents the presence ($s_{ji} = 1$) or absence ($s_{ji} = 0$) of a peak summit within the upstream and downstream 100kb centered on TSS. The genome-wide motif scores were scanned at 100bp window size with

the library (https://github.com/qinqian/seqpos2)[71], and the motif hits are defined by thresholding at 99th percentiles then mapped to the 1kb windows. The genome-wide 1kb windows in which the TR peak summits are located were determined using Bedtools[72]. All of the peak-RPs, TR binding and motif hit data were deposited into hdf5 format files.

Lisa framework

Chromatin landscape model

Lisa selects 3000 background genes by proportionally sampling from non-query genes with a range of different TAD and promoter activities based on compendia of Cistrome DB H3K4me3 and H3K27ac ChIP-seq signals. There is no gene ontology enrichment in the background gene set. Lisa then uses L1 regularized logistic regression to select an optimum sample set for H3K27ac ChIP-seq or DNase-seq samples based on R'_{jk}. The L1 penalty parameter is determined by binary search to constrain the number of selected chromatin profiles to be small but sufficient to capture the information (different sample sizes were explored, and ten was used in all the benchmark cases[28]). Lisa trains a final logistic regression model to predict the target gene set, and obtains a weight α_j for each candidate chromatin profile j, from which the weighted sum of chrom-RP is the model regulatory potential (model-RP).

***In silico* deletion (ISD) method**

The rationale for the ISD method is that the peaks of the true regulatory TFs should align with the high chromatin accessibility signals from the corresponding tissue or cell type. Therefore, the computational deletion of the chromatin signals on the peaks of regulatory cistromes would result in a more substantial effect on the model-RP for query genes than for background genes. The regulatory potentials are recalculated after erasing the signal in all 1kb windows containing at least one peak from a putative regulatory cistrome i, $\tilde{R}_{ijk} = R_{jk} - \sum_{m \in M_{ik}} l\, w_m s_{jm}$ (where M_{ik} is the set of 1kb windows containing at least one peak in cistrome i for gene k, l is the window size, which is set to 1kb for this study, w_m is the exponential decay weight with the distance between the mth window center and TSS, the weight function is the same as chrom-RP, s_{jm} is jth average chromatin profile signal on the mth window). These RPs are then normalized using the same normalization factors from the original RPs $\tilde{R}'_{ijk} = \log\left(\tilde{R}_{ijk} + 1\right) - \frac{1}{K}\sum_1^K\left(\log\left(R_{jk} + 1\right)\right)$.

After deletion, the model RPs are recalculated using the weights from the logistic regression model from chromatin profile feature selection without refitting and subtracted from the non-

deletion model-RP, producing a ΔRP value for each gene, defined as the linear combination of differences in regulatory potentials: $\Delta R'_{ik} = \sum_j \alpha_j (R'_{jk} - \tilde{R}'_{ijk})$.

Combined statistics method for TR ranking

The peak-RPs or ΔRPs of the query gene set are compared with that of the background gene set through the one-sided Wilcoxon rank-sum test. For ChIP-seq-based methods, peak-RP, DNase-seq and H3K27ac chom-RP are combined to get a robust prediction of the TRs. For motif-based methods, DNase-seq and H3K27ac ΔRPs are combined to get the final inference of TRs. Both combination of statistics follows the Cauchy combination test[38], in which the combined statistics for each TR is $t_j = \sum_{i=1}^{d} w_i \tan\{(0.5 - p_i)\pi\}$, j represents one TR, i represents ith method within ChIP-seq-based or motif-based methods, p_i is the corresponding p-value, w_i is set to 1/d where d is 3 for ChIP-seq-based method or 2 for the motif-based method. The combined p-value for a TR j is computed as $p_j = 1/2 - (\arctan(t_j))/\pi$.

Baseline method

The baseline method, which is "peaks in promoter" for ChIP-seq based method or "hits in promoter" for the motif-based method, is implemented by counting the number of TF ChIP-seq binding summits or motif hits within the genomic interval from 5kb upstream to 5kb downstream of the TSS. The peaks or motif counts in the promoter of target gene set are compared with that of the background gene set using the one-sided Wilcoxon rank-sum test.

Comparison of "direct" and "indirect" binding sites

For up- and down-regulated gene sets from the same experiment, the peaks of the target TR ChIP-seq samples with the most significant p-values are defined as "direct" or "indirect" binding sites based on the target TR motif scores. Peak-RPs of "direct" or "indirect" binding sites are calculated and normalized to percentiles. Statistical significance between query and background gene sets was calculated by the one-sided Wilcoxon rank sum test.

Comparison of Lisa with published methods

All up- and down-regulated gene sets in Lisa's benchmark dataset were also used to test other published methods. BART and ICistargets were manually run through the online websites with the default settings. Enrichr was run using the API. When comparing the motif-based methods, PWMs from species other than human or mouse were removed since they are not included in LISA framework.

BART: http://bartweb.org/

ICistargets: https://gbiomed.kuleuven.be/apps/lcb/i-cisTarget/?ref=labworm

Enrichr: http://amp.pharm.mssm.edu/Enrichr/

Lisa pipeline

The Lisa pipeline is implemented with Snakemake[73]. Lisa contains an interface to process FASTQ format files to BigWig format files, and to generates hdf5 files containing the chrom-RP matrices and 1kb resolution data required by the Lisa model module.

Lisa online application

We have implemented the online version of Lisa (http://lisa.cistrome.org) using the Flask Python web development framework, along with process control software Celery to queue numerous queries. The analysis result of the target gene set is closely linked to the Cistrome DB. The scatterplot comparing TR ranking results from a pair of query gene sets such as up- and down-regulated gene sets is implemented in Plot.ly.

Funding

This work was supported by grants from the NIH (U24 HG009446 to XLS, U24 CA237617 to XSL and CAM), National Natural Science Foundation of China (31801110 to S.M.) and the Shanghai Sailing Program (18YF1402500 to QQ).

References

1. Hanahan, D. & Weinberg, R. A. Hallmarks of cancer: the next generation. *Cell* **144**, 646–674 (2011).
2. Takahashi, K. & Yamanaka, S. Induction of Pluripotent Stem Cells from Mouse Embryonic and Adult Fibroblast Cultures by Defined Factors. *Cell* **126**, 663–676 (2006).
3. Thurman, R. E. *et al.* The accessible chromatin landscape of the human genome. *Nature* **489**, 75–82 (2012).
4. Gerstein, M. B. *et al.* Architecture of the human regulatory network derived from ENCODE data. *Nature* **488**, 91–100 (2012).
5. Creyghton, M. P. *et al.* Histone H3K27ac separates active from poised enhancers and predicts developmental state. *Proc. Natl. Acad. Sci. U. S. A.* **107**, 21931–6 (2010).
6. Heinz, S. *et al.* Simple combinations of lineage-determining transcription factors prime cis-

regulatory elements required for macrophage and B cell identities. *Mol. Cell* **38**, 576–89 (2010).

7. He, H. H. *et al.* Nucleosome dynamics define transcriptional enhancers. *Nat. Genet.* **42**, 343–7 (2010).
8. Mikkelsen, T. S. *et al.* Genome-wide maps of chromatin state in pluripotent and lineage-committed cells. *Nature* **448**, 553–60 (2007).
9. Johnson, D. S., Mortazavi, A., Myers, R. M. & Wold, B. *Genome-wide mapping of in vivo protein-DNA interactions. Science (New York, N.Y.)* **316**, (2007).
10. Lambert, S. A. *et al.* The Human Transcription Factors. *Cell* **172**, 650–665 (2018).
11. Fulton, D. L. *et al.* TFCat: the curated catalog of mouse and human transcription factors. *Genome Biol.* **10**, R29 (2009).
12. Mei, S. *et al.* Cistrome Data Browser: a data portal for ChIP-Seq and chromatin accessibility data in human and mouse. *Nucleic Acids Res.* **45**, D658–D662 (2017).
13. ENCODE. An integrated encyclopedia of DNA elements in the human genome. *Nature* **489**, 57–74 (2012).
14. Savic, D. *et al.* CETCh-seq: CRISPR epitope tagging ChIP-seq of DNA-binding proteins. *Genome Res.* **25**, 1581–1589 (2015).
15. Skene, P. J. & Henikoff, S. An efficient targeted nuclease strategy for high-resolution mapping of DNA binding sites. *Elife* (2017). doi:10.7554/eLife.21856
16. Hesselberth, J. R. *et al.* Global mapping of protein-DNA interactions in vivo by digital genomic footprinting. **6**, 283–289 (2009).
17. Boyle, A. P. *et al.* High-resolution genome-wide in vivo footprinting of diverse transcription factors in human cells. *Genome Res.* **21**, 456–64 (2011).
18. Buenrostro, J. D., Giresi, P. G., Zaba, L. C., Chang, H. Y. & Greenleaf, W. J. Transposition of native chromatin for fast and sensitive epigenomic profiling of open chromatin , DNA-binding proteins and nucleosome position. *Nat. Methods* 1–8 (2013). doi:10.1038/nmeth.2688
19. Rada-Iglesias, A. *et al.* A unique chromatin signature uncovers early developmental enhancers in humans. *Nature* **470**, 279–83 (2011).
20. Meyer, C. A., He, H. H., Brown, M. & Liu, X. S. BINOCh: Binding inference from nucleosome occupancy changes. *Bioinformatics* **27**, 1867–1868 (2011).
21. He, H. H. *et al.* Differential DNase I hypersensitivity reveals factor-dependent chromatin dynamics. *Genome Res.* **22**, 1015–25 (2012).
22. Keilwagen, J., Posch, S. & Grau, J. Accurate prediction of cell type-specific transcription

572 factor binding. *Genome Biol.* **20**, 1–17 (2019).
573 23. Schreiber, J., Bilmes, J. & Noble, W. S. Completing the ENCODE3 compendium yields
574 accurate imputations across a variety of assays and human biosamples. 1–20 (2019).
575 24. Qin, Q. & Feng, J. Imputation for transcription factor binding predictions based on deep
576 learning. *PLOS Comput. Biol.* **13**, e1005403 (2017).
577 25. Li, H., Quang, D. & Guan, Y. Anchor : trans-cell type prediction of transcription factor binding
578 sites. 281–292 (2019). doi:10.1101/gr.237156.118.29
579 26. Karimzadeh, M. & Hoffman, M. M. Virtual ChIP-seq : predicting transcription factor binding
580 by learning from the transcriptome. (2018).
581 27. Quang, D. & Xie, X. FactorNet : a deep learning framework for predicting cell type specific
582 transcription factor binding from nucleotide-resolution sequential data. 1–27 (2017).
583 28. Wang, S. *et al.* Modeling cis-regulation with a compendium of genome-wide histone
584 H3K27ac profiles. *Genome Res.* **26**, 1417–1429 (2016).
585 29. Wang, Z. *et al.* BART: a transcription factor prediction tool with query gene sets or
586 epigenetic profiles. *Bioinformatics* 0–2 (2018). doi:10.1093/bioinformatics/bty194
587 30. Imrichova, H., Hulselmans, G., Atak, Z. K., Potier, D. & Aerts, S. I-cisTarget 2015 update:
588 Generalized cis-regulatory enrichment analysis in human, mouse and fly. *Nucleic Acids*
589 *Res.* **43**, W57–W64 (2015).
590 31. Kuleshov, M. V *et al.* Enrichr: a comprehensive gene set enrichment analysis web server
591 2016 update. *Nucleic Acids Res.* **44**, W90-7 (2016).
592 32. Long, H. K., Prescott, S. L. & Wysocka, J. Ever-Changing Landscapes: Transcriptional
593 Enhancers in Development and Evolution. *Cell* **167**, 1170–1187 (2016).
594 33. Osterwalder, M. *et al.* Enhancer redundancy provides phenotypic robustness in
595 mammalian development. *Nature* (2018). doi:10.1038/nature25461
596 34. Fukaya, T., Lim, B. & Levine, M. Enhancer Control of Transcriptional Bursting. *Cell* **166**,
597 358–368 (2016).
598 35. Ouyang, Z., Zhou, Q. & Hung, W. ChIP-Seq of transcription factors predicts absolute and
599 differential gene expression in embryonic stem cells. (2009).
600 36. Wang, S. *et al.* Target analysis by integration of transcriptome and ChIP-seq data with
601 BETA. *Nat. Protoc.* **8**, 2502–2515 (2013).
602 37. Sikora-Wohlfeld, W., Ackermann, M., Christodoulou, E. G., Singaravelu, K. & Beyer, A.
603 Assessing computational methods for transcription factor target gene identification based
604 on ChIP-seq data. *PLoS Comput. Biol.* **9**, e1003342 (2013).
605 38. Liu, Y. & Xie, J. Cauchy combination test: a powerful test with analytic p-value calculation

606 under arbitrary dependency structures. (2018).
607 39. Chia, N. Y. *et al.* Regulatory crosstalk between lineage-survival oncogenes KLF5, GATA4
608 and GATA6 cooperatively promotes gastric cancer development. *Gut* (2015).
609 doi:10.1136/gutjnl-2013-306596
610 40. Yang, X. Z. *et al.* LINC01133 as ceRNA inhibits gastric cancer progression by sponging
611 miR-106a-3p to regulate APC expression and the Wnt/β-catenin pathway. *Mol. Cancer*
612 (2018). doi:10.1186/s12943-018-0874-1
613 41. Hwang, J. T. K. & Kelly, G. M. GATA6 and FOXA2 Regulate Wnt6 Expression During
614 Extraembryonic Endoderm Formation. *Stem Cells Dev.* **21**, 3220–3232 (2012).
615 42. Weidenfeld, J., Shu, W., Zhang, L., Millar, S. E. & Morrisey, E. E. The WNT7b promoter is
616 regulated by TTF-1, GATA6, and Foxa2 in lung epithelium. *J. Biol. Chem.* **277**, 21061–
617 21070 (2002).
618 43. Muzikar, K. A., Nickols, N. G. & Dervan, P. B. Repression of DNA-binding dependent
619 glucocorticoid receptor-mediated gene expression. **2009**, (2009).
620 44. Alvarez, M. J. *et al.* Functional characterization of somatic mutations in cancer using
621 network-based inference of protein activity. *Nat. Genet.* (2016). doi:10.1038/ng.3593
622 45. Fiaschetti, G. *et al.* Bone morphogenetic protein-7 is a MYC target with prosurvival
623 functions in childhood medulloblastoma. *Oncogene* (2011). doi:10.1038/onc.2011.10
624 46. Vencken, S. F. *et al.* An integrated analysis of the SOX2 microRNA response program in
625 human pluripotent and nullipotent stem cell lines. *BMC Genomics* (2014).
626 doi:10.1186/1471-2164-15-711
627 47. Ci, W. *et al.* The BCL6 transcriptional program features repression of multiple oncogenes
628 in primary B cells and is deregulated in DLBCL. *Blood* (2009). doi:10.1182/blood-2008-12-
629 193037
630 48. Parekh, S. *et al.* BCL6 programs lymphoma cells for survival and differentiation through
631 distinct biochemical mechanisms. *Blood* **110**, 2067–2074 (2007).
632 49. Huynh, K. D. & Bardwell, V. J. The BCL-6 POZ domain and other POZ domains interact
633 with the co-repressors N-CoR and SMRT. *Oncogene* **17**, 2473–2484 (1998).
634 50. Cui, J. *et al.* FBI-1 functions as a novel AR co-repressor in prostate cancer cells. *Cell. Mol.*
635 *Life Sci.* (2011). doi:10.1007/s00018-010-0511-7
636 51. Wei, F., Zaprazna, K., Wang, J. & Atchison, M. L. PU.1 Can Recruit BCL6 to DNA To
637 Repress Gene Expression in Germinal Center B Cells. *Mol. Cell. Biol.* **29**, 4612–4622
638 (2009).
639 52. Huynh, K. D., Fischle, W., Verdin, E. & Bardwell, V. J. BCoR, a novel corepressor involved

in BCL-6 repression. *Genes Dev.* (2000). doi:10.1111/j.1754-7121.1984.tb00653.x

53. Grandori, C., Cowley, S. M., James, L. P. & Eisenman, R. N. The Myc/Max/Mad Network and the Transcriptional Control of Cell Behavior. *Annu. Rev. Cell Dev. Biol.* (2000). doi:10.1146/annurev.cellbio.16.1.653

54. Tzatsos, A. *et al.* KDM2B promotes pancreatic cancer via Polycomb-dependent and -independent transcriptional programs. *J. Clin. Invest.* (2013). doi:10.1172/JCI64535

55. Andoniadou, C. L. *et al.* Sox2+stem/progenitor cells in the adult mouse pituitary support organ homeostasis and have tumor-inducing potential. *Cell Stem Cell* **13**, 433–445 (2013).

56. Friedman, J. R. & Kaestner, K. H. The Foxa family of transcription factors in development and metabolism. *Cellular and Molecular Life Sciences* (2006). doi:10.1007/s00018-006-6095-6

57. Chen, T. *et al.* Foxa1 contributes to the repression of Nanog expression by recruiting Grg3 during the differentiation of pluripotent P19 embryonal carcinoma cells. **6**, (2014).

58. Hagey, D. W. *et al.* SOX2 regulates common and specific stem cell features in the CNS and endoderm derived organs. *PLoS Genet.* (2018). doi:10.1371/journal.pgen.1007224

59. Teo, A. K. K. *et al.* Pluripotency factors regulate definitive endoderm specification through eomesodermin. *Genes Dev.* (2011). doi:10.1101/gad.607311

60. Segal, E. *et al.* Module networks: identify regulatory modules and their condition-specific regulators from gene expression data. *Nat. Genet.* **34**, 166–176 (2003).

61. Carroll, J. S., Prall, O. W. J., Musgrove, E. A. & Sutherland, R. L. A pure estrogen antagonist inhibits cyclin E-Cdk2 activity in MCF-7 breast cancer cells and induces accumulation of p130-E2F4 complexes characteristic of quiescence. *J. Biol. Chem.* **275**, 38221–38229 (2000).

62. Li, D., Hsu, S., Purushotham, D., Sears, R. L. & Wang, T. WashU Epigenome Browser update 2019. *Nucleic Acids Res.* (2019). doi:10.1093/nar/gkz348

63. Shang, Y., Hu, X., DiRenzo, J., Lazar, M. A. & Brown, M. Cofactor Dynamics and Sufficiency in Estrogen Receptor–Regulated Transcription. *Cell* **103**, 843–852 (2000).

64. Vockley, C. M. *et al.* Direct GR Binding Sites Potentiate Clusters of TF Binding across the Human Genome Direct GR Binding Sites Potentiate Clusters of TF Binding across the Human Genome. *Cell* **166**, 1269-1281.e19 (2016).

65. Crow, M., Lim, N., Ballouz, S., Pavlidis, P. & Gillis, J. Predictability of human differential gene expression. *Proc. Natl. Acad. Sci. U. S. A.* **116**, 6491–6500 (2019).

66. Muhar, M. *et al.* SLAM-seq defines direct gene-regulatory functions of the BRD4-MYC axis. *Science (80-.).* **360**, 800–805 (2018).

67. Aibar, S. *et al.* SCENIC : single-cell regulatory network inference and clustering. **14**, (2017).
68. Kent, W. J., Zweig, A. S., Barber, G., Hinrichs, A. S. & Karolchik, D. BigWig and BigBed: enabling browsing of large distributed datasets. *Bioinformatics* **26**, (2010).
69. Matys, V. *et al.* TRANSFAC®: Transcriptional regulation, from patterns to profiles. *Nucleic Acids Res.* **31**, 374–378 (2003).
70. Mathelier, A. *et al.* JASPAR 2016 : a major expansion and update of the open-access database of transcription factor binding. **44**, 110–115 (2016).
71. Liu, T. *et al.* Cistrome: an integrative platform for transcriptional regulation studies. *Genome Biol.* **12**, R83 (2011).
72. Quinlan, A. R. & Hall, I. M. BEDTools: a flexible suite of utilities for comparing genomic features. *Bioinformatics* **26**, 841–842 (2010).
73. Köster, J. & Rahmann, S. Snakemake--a scalable bioinformatics workflow engine. *Bioinformatics* **28**, 2520–2 (2012).

Figures

Fig. 1. Illustration of the Lisa framework. (**a**) The peak-RP score models the effect of TR binding sites on the regulation of a gene. TR binding sites are binary values and peaks nearer to the gene's TSS have a greater influence than ones further away. (**b**) The chrom-RP score summarizes the effect of the DNase-seq or H3K27ac chromatin environment on a gene. The chrom-RP score is based on a continuous rather than binary signal quantification. (**c**) Overview of the Lisa framework. (**1**) H3K27ac ChIP-seq or DNase-seq data from the Cistrome DB is summarized using the chrom-RP score for each gene. (**2**) H3K27ac ChIP-seq or DNase-seq samples that can discriminate between the query gene set and the background gene set are selected and the regression parameters define a chrom-RP model. (**3**) Each TR cistrome from the Cistrome DB is evaluated as a putative regulator of the query gene set through *in silico* deletion, which involves the elimination of H3K27ac ChIP-seq or DNase-seq signal at the binding sites of the putative regulator. (**4**) The chrom-RP model, based on *in silico* deletion signal, is compared to the model without deletion for each gene in the query and background gene sets. A p-value is calculated using the Wilcoxon rank test comparison of the query and background ΔRPs. (**5**) The peak-RP based on TR ChIP-seq peaks is calculated for the putative regulatory cistrome and the statistical significance of peak-RP distributions from the query and background gene sets is calculated. (**6**) p-values from the H3K27ac ChIP-seq, DNase-seq and peak-RP analysis are combined using the

706 Cauchy combination test. TR cistromes are ranked based on the combined p-value.

707 **Fig. 2.** A down-regulated gene set from a GATA6 knock-down experiment in gastric cancer KATO-
708 III cells is used as a case study to demonstrate the Lisa framework. (**a**) Heatmap of regulatory
709 potentials used to discriminate down-regulated genes from non-regulated background genes. (**b**)
710 *In silico* deletion analysis using GATA6 and CTCF cistromes to probe chromatin landscape
711 models near an illustrative down-regulated gene, LINC01133 and a background gene ZC3H12A.
712 Only the H3K27ac ChIP-seq and DNase-seq chromatin profiles with the largest positive
713 coefficients are shown, although other samples contribute to the respective H3K27ac ChIP-seq
714 and DNase-seq chromatin models. (**c**) Comparison of ΔRPs indicates GATA6 and GATA4
715 cistromes have a large impact on the chromatin landscapes near down-regulated genes, and are
716 therefore likely to be regulators of the query gene set. CTCF does not influence the chromatin
717 landscape of the down-regulated genes and is not likely to regulate the query gene set. (**d**) The
718 rank statistics for the Lisa analysis of the down-regulated gene set in the GATA6 knockdown
719 experiment were combined to get overall TR ranks. The top 8 and bottom 8 TRs for all TR ChIP-
720 seq samples are shown.

721 **Fig. 3**. Lisa predicts key transcriptional regulators and assigns significance to each Cistrome DB
722 cistrome. The large heatmap shows the hierarchical clustering of 8,471 human Cistrome DB
723 ChIP-seq cistromes based on peak-RP, with color representing Pearson correlation coefficients
724 between peak-RPs. The three bars to the left of the heatmap display Lisa significance scores for
725 differentially expressed genes sets derived from GR activation in the A549 cell line (up-regulated),
726 GATA6 knock-down in gastric cancer (down-regulated) and AR activation in the LNCaP cell line
727 (up-regulated). Small heatmaps show details of the global heatmap relevant to (**a**) AR activation,
728 (**b**) GATA6 knock-down, and (**c**) GR activation gene sets. In each case the most significant
729 cistromes are derived from the same cell type or lineage.
730
731 **Fig. 4.** Lisa can accurately identify key transcriptional regulators and coregulators using Cistrome
732 DB cistromes. Lisa analyses of up- and down-regulated gene sets from (**a**) GR over-expression,
733 (**b**) BCL6 knock-down, (**c**) MYC knock-down and (**d**) SOX2 knock-out experiments. The scatter
734 plots show negative $\log_{10}$ Lisa p-values of 1316 unique transcriptional regulators for up- and down-
735 regulated gene sets. Colors indicates $\log_2$ fold changes of the TF gene expression between
736 treatment and control conditions in the gene expression experiment. Dots outlined with a circle
737 denote transcriptional regulators that physically interact with the TF perturbed in the experiment,

which is marked with a cross.

Fig. 5. Systematic evaluation of regulator prediction performance for human using Cistrome DB ChIP-seq and DNA motif derived cistromes. (**a**) Heatmap showing Lisa performance in the analysis of human TF perturbation experiments. Each column represents a TF activation/over-expression or knock-down/out experiment with similar experiment types grouped together. Rows represent methods based on cistromes from TR ChIP-seq data or imputed from motifs. The upper left red triangles represent the rank of the target TFs based on the analysis of the up-regulated gene sets; the lower right blue triangles represent analysis of down-regulated gene sets. The heatmap includes non-redundant human experiments for the same TF. See Supplementary Fig. 5 for the complete list of human and mouse experiments. (**b**) Boxplot showing the target TF rankings comparing Lisa ChIP-seq based methods and the baseline model based on TF peak counts in gene promoter regions to analyze up- and down-regulated gene sets in over-expression/activation (OE) and knock-down/out experiments (KD/KO). (**c**) Boxplot showing target TF rankings using Lisa motif-based methods and the baseline model based on motif hits in promoter regions.

Fig. 6. Lisa performance surpasses published models. Lisa performance is compared with alternative published methods for (**a**) up-regulated genes in over-expression/activation experiments and (**b**) down-regulated genes in knock-down/out experiments.

Supplementary Fig. 1. Catalog of chromatin and cistrome profiles integrated in the Lisa framework. (**a**) Stacked bar plot showing the Cistrome DB (version 1) chromatin profile sample numbers in major cell types for human and mouse. Histogram showing the numbers of cell lines in which TFs in the Cistrome DB are represented by ChIP-seq samples for (**b**) human, and (**c**) mouse. (**d**) Heatmap displaying the ChIP-seq sample number for each of the TR - cell line combinations. The color represents the sample number.

Supplementary Fig. 2. Lisa chromatin landscape model evaluation for the down-regulated gene set from a GATA6 knock-down experiment in gastric cancer. (**a**) ROC curve for the performance of the classifier in discriminating the target gene set from a background gene set based on DNase-seq. (**b**) DNase-seq samples selected from the Cistrome DB and the associated logistic regression coefficients. (**c**) ROC curve for the performance of the classifier in discriminating the target gene set from a background gene set based on H3K27ac ChIP-seq. (**d**) H3K27ac ChIP-

seq samples selected from the Cistrome DB and the associated logistic regression coefficients.

Supplementary Fig. 3. Lisa predicts key transcriptional regulators and assigns significance to Cistrome DB cistromes. The large heatmap shows the hierarchical clustering of 8,471 transcriptional regulators based on peak-RP derived from Cistrome DB ChIP-seq cistromes, with color representing Pearson correlation coefficients between peak-RPs. The two bars on the left represent Lisa significance scores from SOX2 and POU5F1 perturbation experiments. A detail heatmap showing the clusters of samples enriched around the significant TFs include SOX2, POU5F1, NANOG, CTNNB1 and SMAD3.

Supplementary Fig. 4. Additional cases showing that Lisa can accurately infer TRs and coregulators using Cistrome DB cistromes. Lisa analysis for up- and down-regulated gene sets from (**a**) POU5F1 knock-down, (**b**) KLF5 knock-down, (**c**) NFE2L2 knock-down. The scatter plots show negative $\log_{10}$ Lisa p-values of 1316 unique transcriptional regulators for up- and down-regulated gene sets. Color indicates $\log_2$ fold change of the TF gene expression between treatment and control conditions in the gene expression experiment. Dots outlined with a circle denote transcriptional regulators that physically interact with the target TF, which is marked with a cross. (**d**) Radar plot of cofactors discovered along with the target TFs grouped by TF perturbation. The top ranked TFs are at the perimeter and the lowest ranked are at the center. The blue and red curves represent the ranks of interactors in the Lisa analysis for down- and up-regulated gene sets, respectively.

Supplementary Fig. 5. Systematic application of Lisa to large-scale transcriptional regulator perturbation study reveals novel recurring regulatory patterns for both human and mouse. (**a-b**) Heatmap showing that Lisa is capable of predicting most of the TF perturbation benchmark gene sets based on cistrome profiles for (**a**) human and (**b**) mouse. Each column represents a TF activation/over-expression or knock-down/out experiment with similar experiment types grouped together. Rows represent Lisa methods based on cistromes from TR ChIP-seq data or imputed from motifs. The upper left red triangles represent the rank of the target TFs based on the analysis of the up-regulated gene sets; the lower right blue triangles represent analysis of down-regulated gene sets. The heatmap contains all of the gene sets used in the evaluation. (**c-d**) the ROC AUC metrics for the Lisa chromatin model for predicting the target gene set from TF perturbation benchmark datasets in (**c**) human and (**d**) mouse. (**e**) Boxplots showing mouse benchmark dataset performance of Lisa ChIP-seq based models and the baseline model based on TF peak

806 counts in gene promoter regions. (**f**) Boxplots showing mouse benchmark datasets performance
807 of Lisa motif-based methods and the baseline model based on motif hits in promoter regions.
808
809 **Supplementary Fig. 6.** Comparison of direct and indirect binding sites in ER and GR activation
810 experiments. Direct binding sites are defined as ChIP-seq peaks with the cognate TR motif and
811 the indirect binding sites are defined as the peaks without the motif. Peak-RPs calculated based
812 on direct and indirect peaks are compared between query and background gene sets.
813
814 **Supplementary Table 1**: Cistrome profile annotation table including TR ChIP-seq and TF motifs
815 **Supplementary Table 2**: DNase-seq and H3K27ac sample annotation table for mouse and
816 human
817 **Supplementary Table 3**: Analysis of Lisa predictions of GR and ER regulated genes using data
818 which does not match the specific cell type. The cell line and cell type of the highest ranked Lisa
819 predicted target TR sample are shown in parentheses in each case.
820 **Supplementary Table 4**: TF perturbation DNA microarray meta table for benchmarking the peak-
821 RP and Lisa methods

Figures

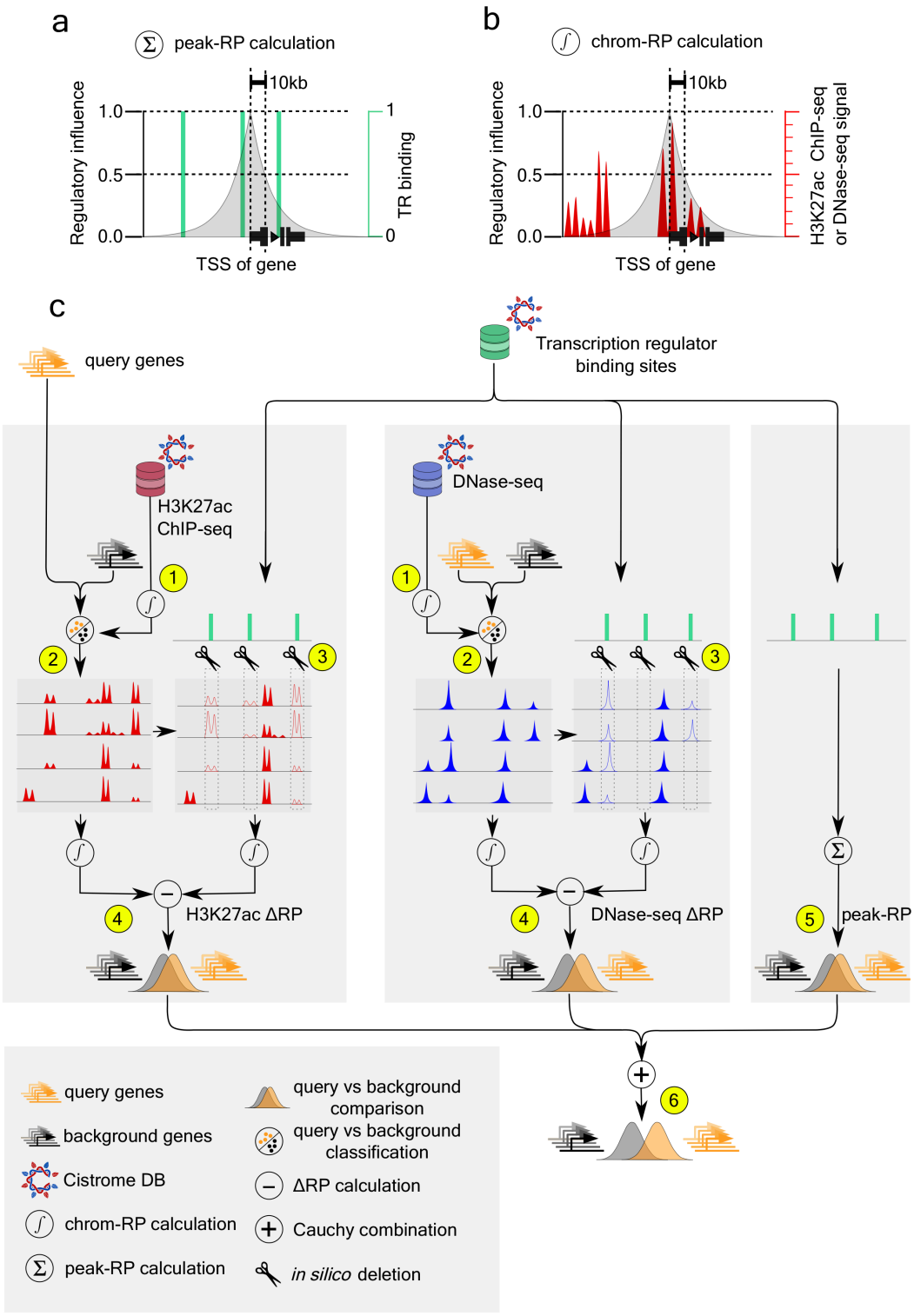

Fig. 1. Illustration of the Lisa framework. (**a**) The peak-RP score models the effect of TR binding sites on the regulation of a gene. TR binding sites are binary values and peaks nearer to the gene's TSS have a greater influence than ones further away. (**b**) The chrom-RP score summarizes the effect of the DNase-seq or H3K27ac chromatin environment on a gene. The chrom-RP score is based on a continuous rather than binary signal quantification. (**c**) Overview of the Lisa framework. (**1**) H3K27ac ChIP-seq or DNase-seq data from the Cistrome DB is summarized using the chrom-RP score for each gene. (**2**) H3K27ac ChIP-seq or DNase-seq samples that can discriminate between the query gene set and the background gene set are selected and the regression parameters define a chrom-RP model. (**3**) Each TR cistrome from the Cistrome DB is evaluated as a putative regulator of the query gene set through *in silico* deletion, which involves the elimination of H3K27ac ChIP-seq or DNase-seq signal at the binding sites of the putative regulator. (**4**) The chrom-RP model, based on *in silico* deletion signal, is compared to the model without deletion for each gene in the query and background gene sets. A p-value is calculated using the Wilcoxon rank test comparison of the query and background ΔRPs. (**5**) The peak-RP based on TR ChIP-seq peaks is calculated for the putative regulatory cistrome and the statistical significance of peak-RP distributions from the query and background gene sets is calculated. (**6**) p-values from the H3K27ac ChIP-seq, DNase-seq and peak-RP analysis are combined using the Cauchy combination test. TR cistromes are ranked based on the combined p-value.

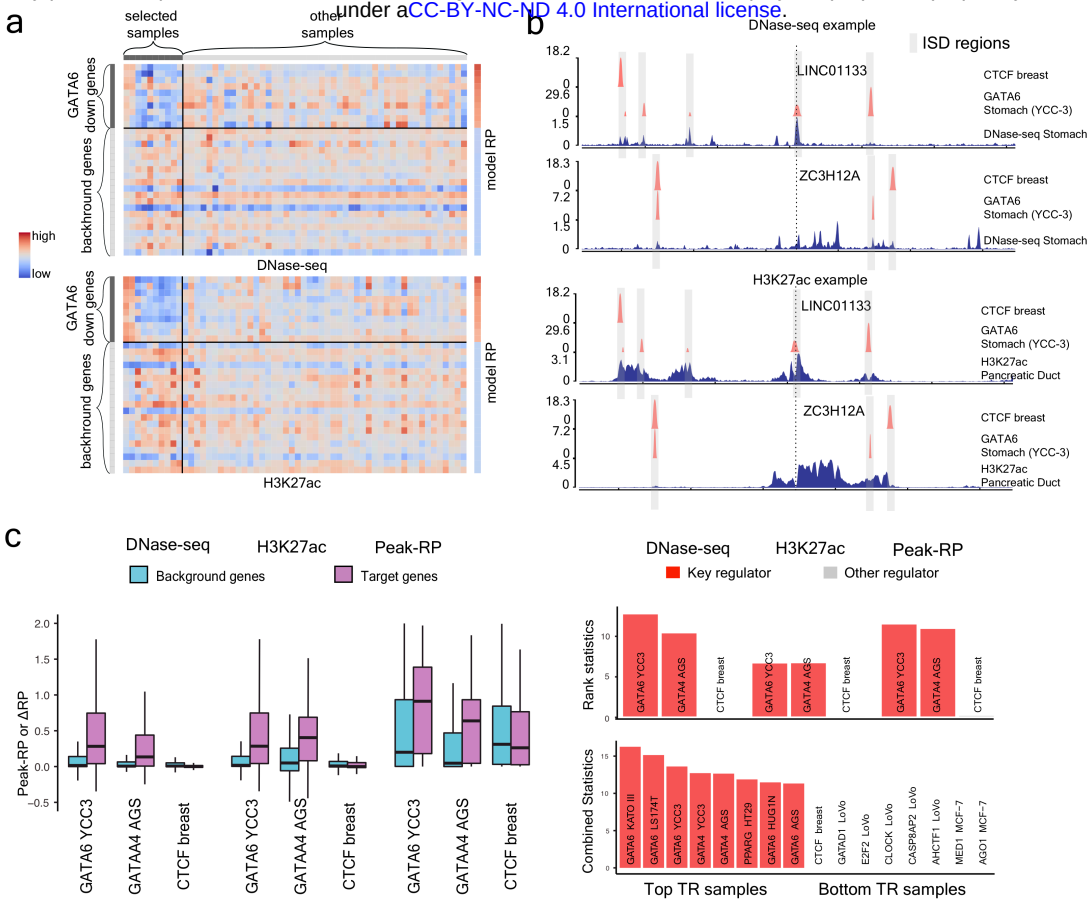

Fig. 2. A down-regulated gene set from a GATA6 knock-down experiment in gastric cancer KATO-III cells is used as a case study to demonstrate the Lisa framework. (**a**) Heatmap of regulatory potentials used to discriminate down-regulated genes from non-regulated background genes. (**b**) *In silico* deletion analysis using GATA6 and CTCF cistromes to probe chromatin landscape models near an illustrative down-regulated gene, LINC01133 and a background gene ZC3H12A. Only the H3K27ac ChIP-seq and DNase-seq chromatin profiles with the largest positive coefficients are shown, although other samples contribute to the respective H3K27ac ChIP-seq and DNase-seq chromatin models. (**c**) Comparison of ΔRPs indicates GATA6 and GATA4 cistromes have a large impact on the chromatin landscapes near down-regulated genes, and are therefore likely to be regulators of the query gene set. CTCF does not influence the chromatin landscape of the down-regulated genes and is not likely to regulate the query gene set. (**d**) The rank statistics for the Lisa analysis of the down-regulated gene set in the GATA6 knockdown experiment were combined to get overall TR ranks. The top 8 and bottom 8 TRs for all TR ChIP-seq samples were shown.

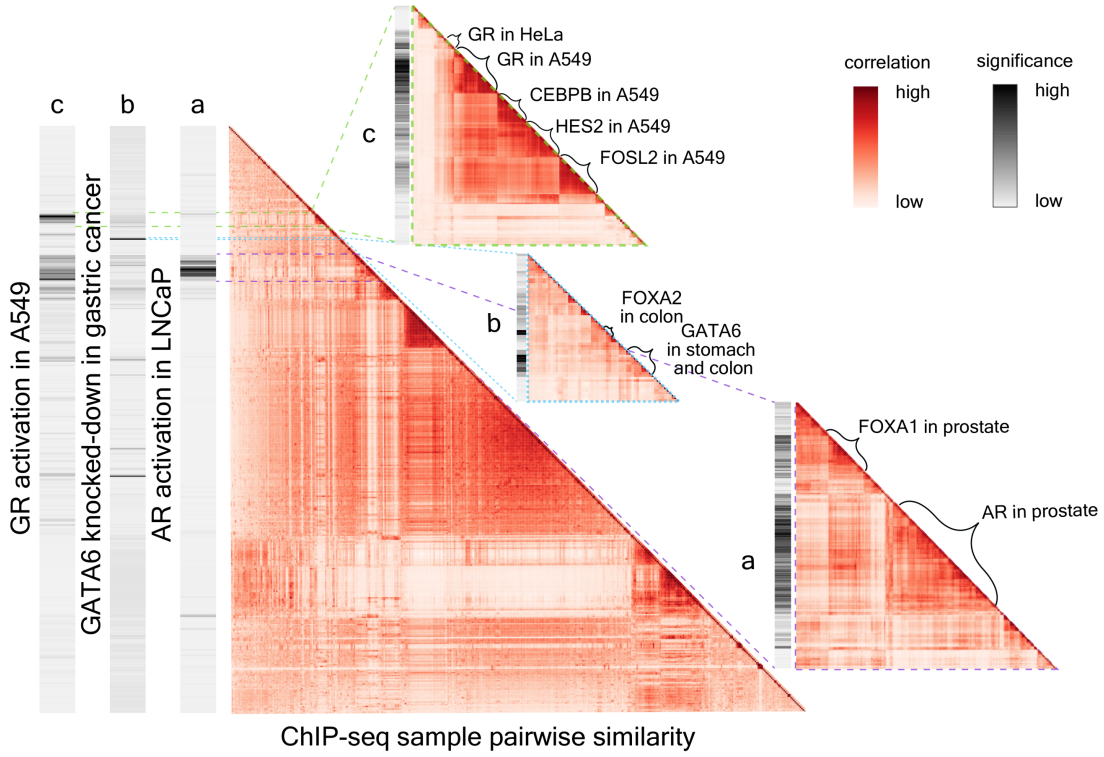

Fig. 3. Lisa predicts key transcriptional regulators and assigns significance to each Cistrome DB cistrome. The large heatmap shows the hierarchical clustering of 8,471 human Cistrome DB ChIP-seq cistromes based on peak-RP, with color representing Pearson correlation coefficients between peak-RPs. The three bars to the left of the heatmap display Lisa significance scores for differentially expressed genes sets derived from GR activation in the A549 cell line (up-regulated), GATA6 knock-down in gastric cancer (down-regulated) and AR activation in the LNCaP cell line (up-regulated). Small heatmaps show details of the global heatmap relevant to (**a**) AR activation, (**b**) GATA6 knock-down, and (**c**) GR activation gene sets. In each case the most significant cistromes are derived from the same cell type or lineage.

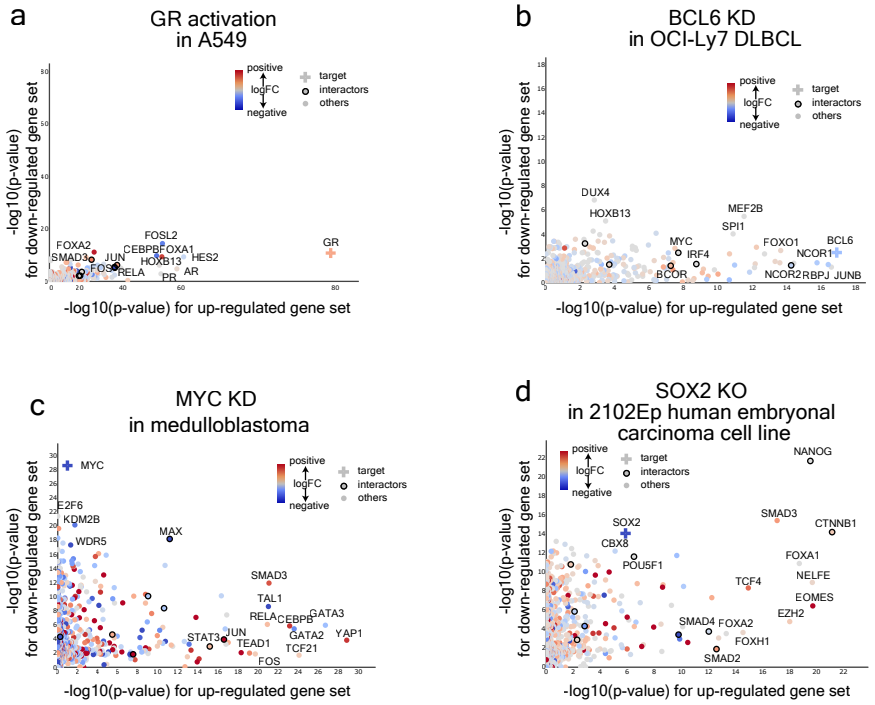

Fig. 4. Lisa can accurately identify key transcriptional regulators and coregulators using Cistrome DB cistromes. Lisa analyses of up- and down-regulated gene sets from (**a**) GR over-expression, (**b**) BCL6 knock-down, (**c**) MYC knock-down and (**d**) SOX2 knock-out experiments. The scatter plots show negative $\log_{10}$ Lisa p-values of 1316 unique transcriptional regulators for up- and down-regulated gene sets. Colors indicates $\log_2$ fold changes of the TF gene expression between treatment and control conditions in the gene expression experiment. Dots outlined with a circle denote transcriptional regulators that physically interact with the TF perturbed in the experiment, which is marked with a cross.

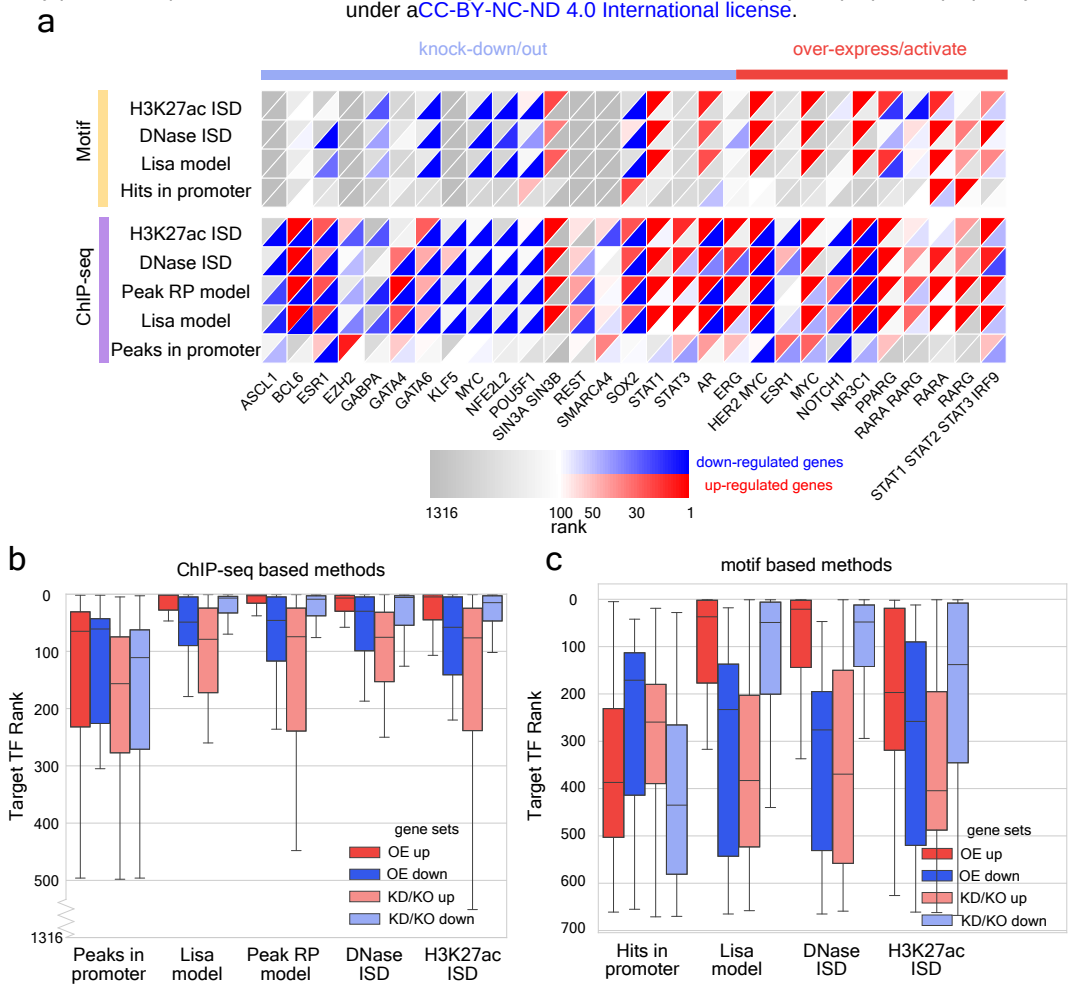

Fig. 5. Systematic evaluation of regulator prediction performance for human using Cistrome DB ChIP-seq and DNA motif derived cistromes. (**a**) Heatmap showing Lisa performance in the analysis of human TF perturbation experiments. Each column represents a TF activation/over-expression or knock-down/out experiment with similar experiment types grouped together. Rows represent methods based on cistromes from TR ChIP-seq data or imputed from motifs. The upper left red triangles represent the rank of the target TFs based on the analysis of the up-regulated gene sets; the lower right blue triangles represent analysis of down-regulated gene sets. The heatmap includes non-redundant human experiments for the same TF. See Supplementary Fig. 5 for the complete list of human and mouse experiments. (**b**) Boxplot showing the target TF rankings comparing Lisa ChIP-seq based methods and the baseline model based on TF peak counts in gene promoter regions to analyze up- and down-regulated gene sets in over-expression/activation (OE) and knock-down/out experiments (KD/KO). (**c**) Boxplot showing target TF rankings using Lisa motif-based methods and the baseline model based on motif hits in promoter regions.

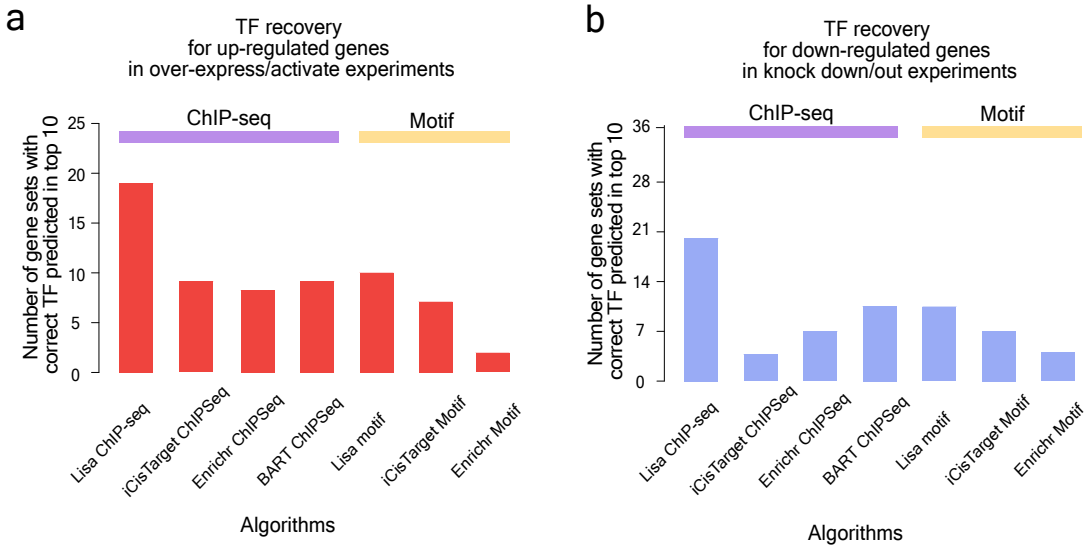

Fig. 6. Lisa performance surpasses published models. Lisa performance is compared with alternative published methods for (**a**) up-regulated genes in over-expression/activation experiments and (**b**) down-regulated genes in knock-down/out experiments.

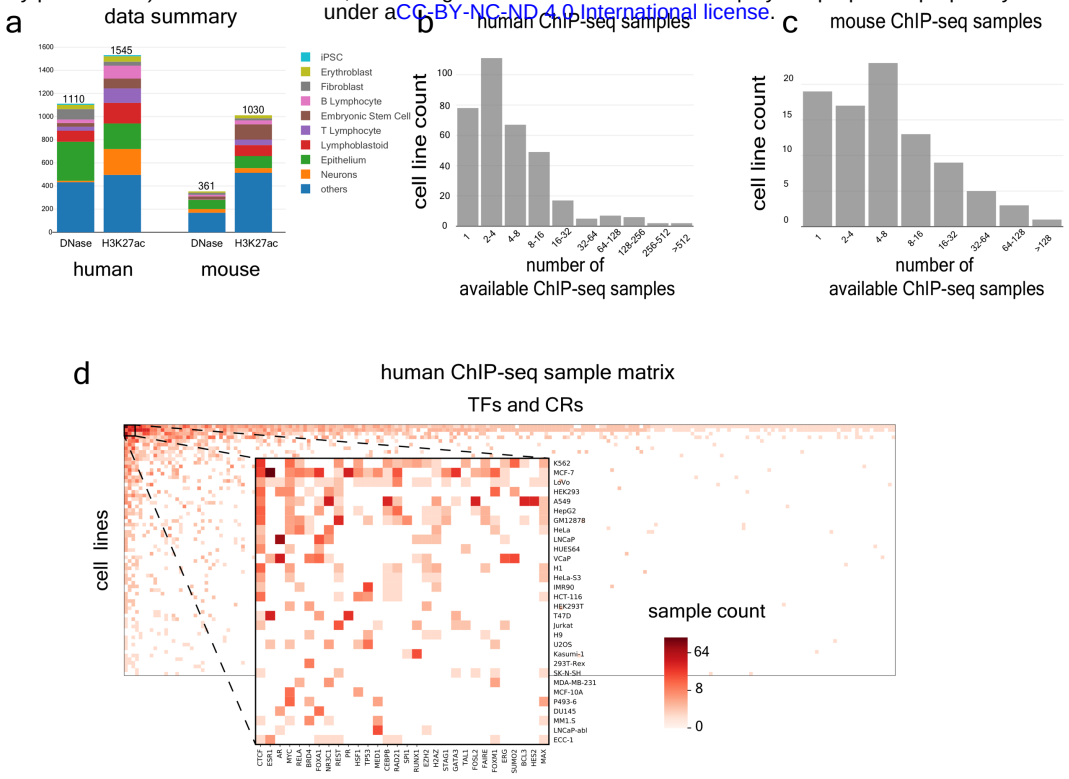

Supplementary Fig. 1. Catalog of chromatin and cistrome profiles integrated in the Lisa framework. (**a**) Stacked bar plot showing the Cistrome DB (version 1) chromatin profile sample numbers in major cell types for human and mouse. Histogram showing the numbers of cell lines in which TFs in the Cistrome DB are represented by ChIP-seq samples for (**b**) human, and (**c**) mouse. (**d**) Heatmap displaying the ChIP-seq sample number for each of the TR - cell line combinations. The color represents the sample number.

a

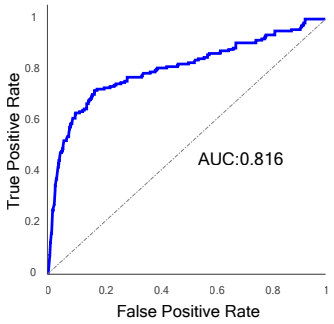

b

DNase

Sample	Model coefficient	Tissue
1	2.11	Stomach
2	0.68	Fetal Large Intestine
3	0.18	Blood
4	0.07	Retina
5	-0.01	Blood
6	-0.19	Bone Marrow
7	-0.20	Blood
8	-0.32	Mammary Gland
9	-0.65	Cord Blood
10	-0.65	Fetal Heart

c

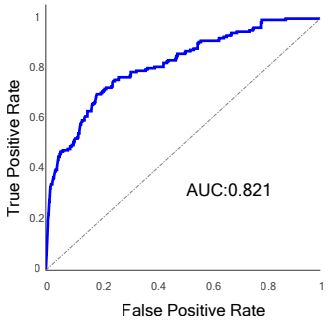

d

H3K27ac

Sample	Model coefficient	Tissue
1	0.65	Fetal Large Intestine
2	0.07	Embryonic Stem Cell
3	0.05	Cerebellum
4	0.02	Blood
5	-0.00	Blood
6	-0.07	Pancreas
7	-0.12	Blood
8	-0.12	Bone Marrow
9	-0.18	Bone Marrow
10	-0.40	Colon

Supplementary Fig. 2. Lisa chromatin landscape model evaluation for the down-regulated gene set from a GATA6 knock-down experiment in gastric cancer. (**a**) ROC curve for the performance of the classifier in discriminating the target gene set from a background gene set based on DNase-seq. (**b**) DNase-seq samples selected from the Cistrome DB and the associated logistic regression coefficients. (**c**) ROC curve for the performance of the classifier in discriminating the target gene set from a background gene set based on H3K27ac ChIP-seq. (**d**) H3K27ac ChIP-seq samples selected from the Cistrome DB and the associated logistic regression coefficients.

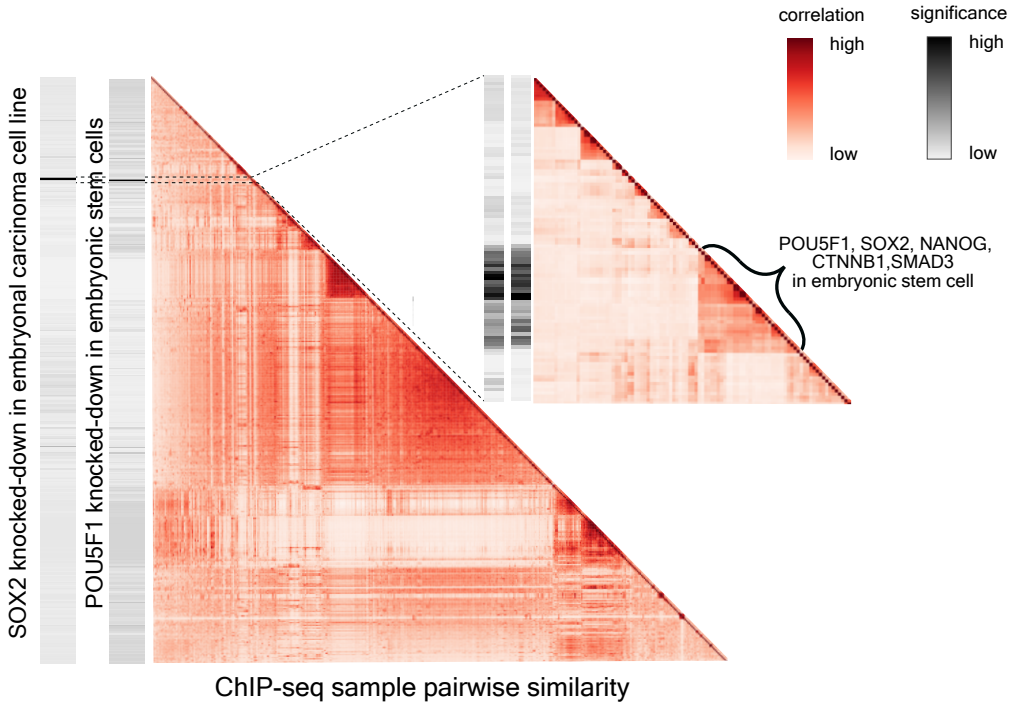

Supplementary Fig. 3. Lisa predicts key transcriptional regulators and assigns significance to Cistrome DB cistromes. The large heatmap shows the hierarchical clustering of 8,471 transcriptional regulators based on peak-RP derived from Cistrome DB ChIP-seq cistromes, with color representing Pearson correlation coefficients between peak-RPs. The two bars on the left represent Lisa significance scores from SOX2 and POU5F1 perturbation experiments. A detail heatmap showing the clusters of samples enriched around the significant TFs include SOX2, POU5F1, NANOG, CTNNB1 and SMAD3.

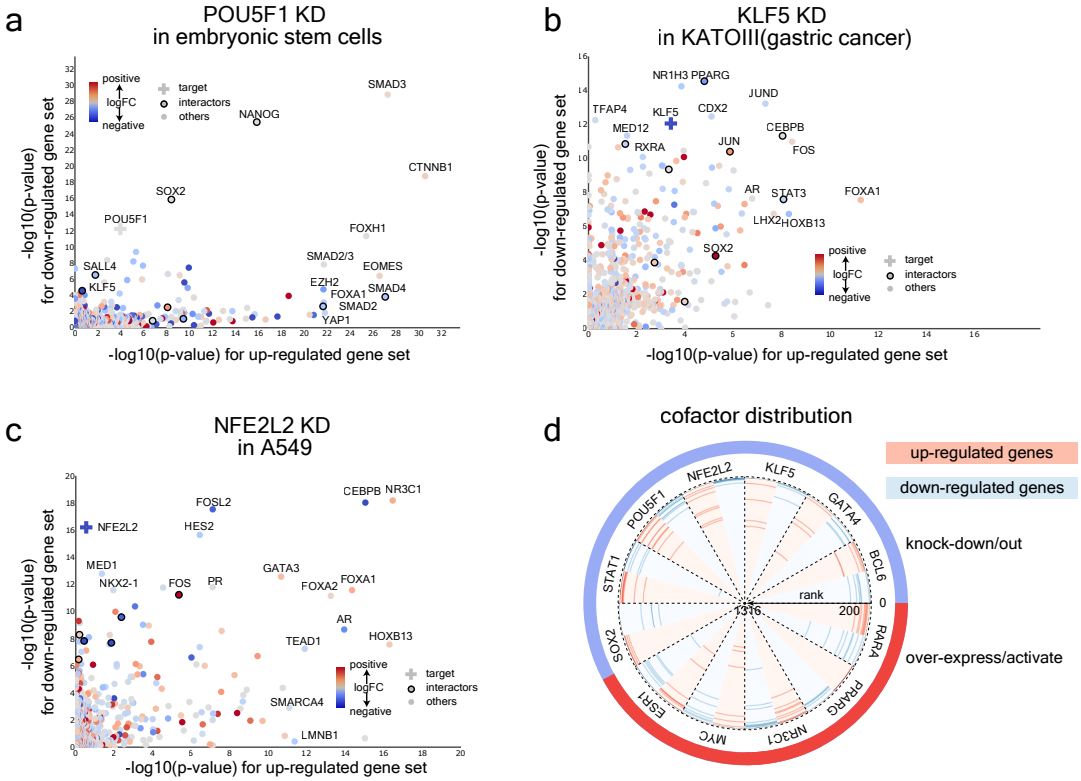

Supplementary Fig. 4. Additional cases showing that Lisa can accurately infer TRs and coregulators using Cistrome DB cistromes. Lisa analysis for up- and down-regulated gene sets from (**a**) POU5F1 knock-down, (**b**) KLF5 knock-down, (**c**) NFE2L2 knock-down. The scatter plots show negative $\log_{10}$ Lisa p-values of 1316 unique transcriptional regulators for up- and down-regulated gene sets. Color indicates $\log_2$ fold change of the TF gene expression between treatment and control conditions in the gene expression experiment. Dots outlined with a circle denote transcriptional regulators that physically interact with the target TF, which is marked with a cross. (**d**) Radar plot of cofactors discovered along with the target TFs grouped by TF perturbation. The top ranked TFs are at the perimeter and the lowest ranked are at the center. The blue and red curves represent the ranks of interactors in the Lisa analysis for down- and up-regulated gene sets, respectively.

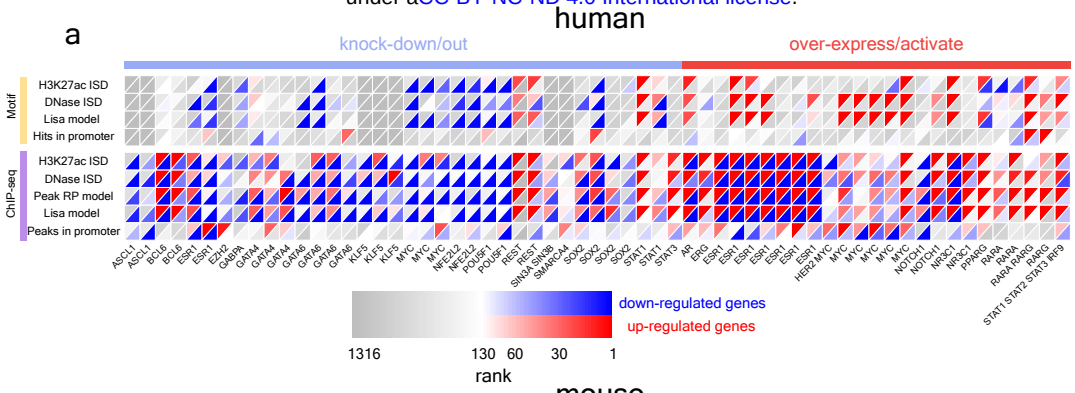

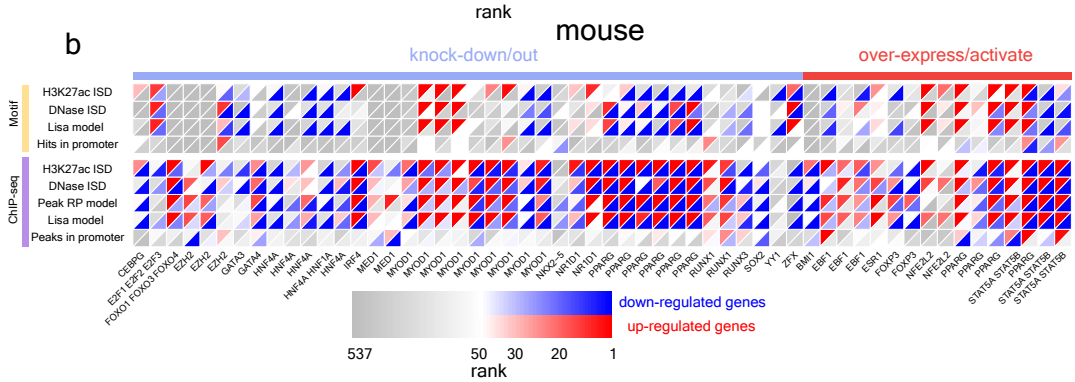

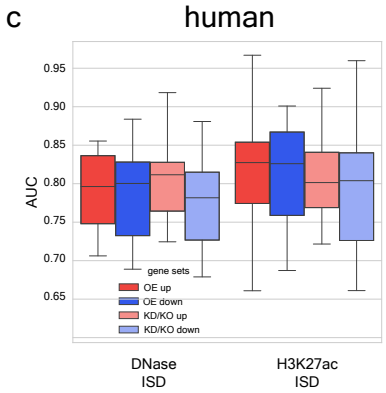

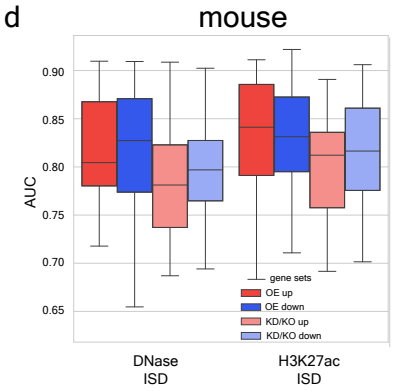

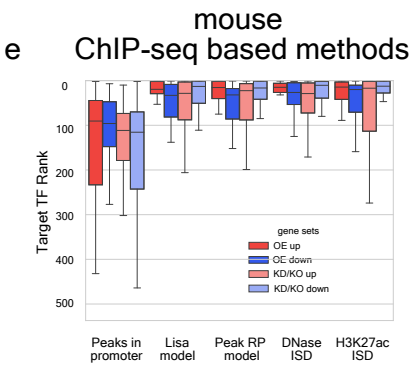

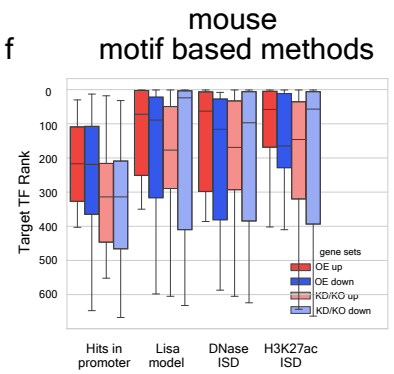

Supplementary Fig. 5. Systematic application of Lisa to large-scale transcriptional regulator perturbation study reveals novel recurring regulatory patterns for both human and mouse. (**a-b**) Heatmap showing that Lisa is capable of predicting most of the TF perturbation benchmark gene sets based on cistrome profiles for (**a**) human and (**b**) mouse. Each column represents a TF activation/over-expression or knock-down/out experiment with similar experiment types grouped together. Rows represent Lisa methods based on cistromes from TR ChIP-seq data or imputed from motifs. The upper left red triangles represent the rank of the target TFs based on the analysis of the up-regulated gene sets; the lower right blue triangles represent analysis of down-regulated gene sets. The heatmap contains all of the gene sets used in the evaluation. (**c-d**) the ROC AUC metrics for the Lisa chromatin model for predicting the target gene set from TF perturbation benchmark datasets in (**c**) human and (**d**) mouse. (**e**) Boxplots showing mouse benchmark dataset performance of Lisa ChIP-seq based models and the baseline model based on TF peak counts in gene promoter regions. (**f**) Boxplots showing mouse benchmark datasets performance of Lisa motif-based methods and the baseline model based on motif hits in promoter regions.

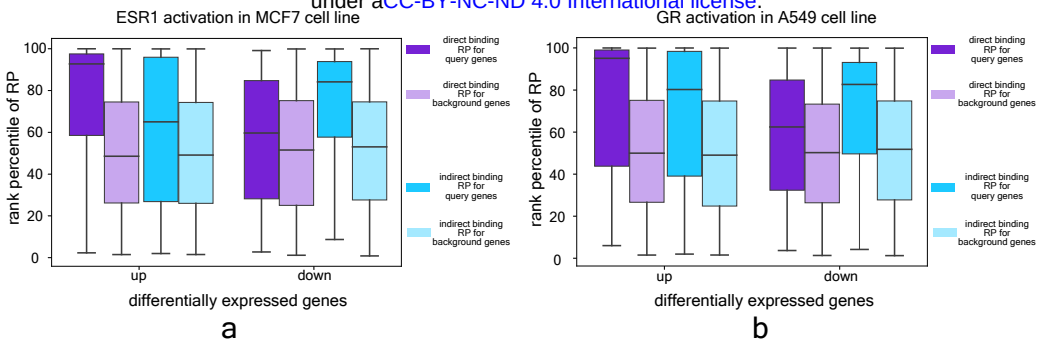

Supplementary Fig. 6. Comparison of direct and indirect binding sites in ER and GR activation experiments. Direct binding sites are defined as ChIP-seq peaks with the cognate TR motif and the indirect binding sites are defined as the peaks without the motif. Peak-RPs calculated based on direct and indirect peaks are compared between query and background gene sets.